LEEM Studies of Epitaxial Nanostructures

E. Bauer and T. Duden

Department of Physics and Astronomy, Arizona State University, Tempe, AZ 85287-1504, USA

(Received: Jan. 31, 1997 Accepted: Feb. 19, 1997)

Abstract

After a brief discussion of the influence of surface diffusion and attachment rates on epitaxial film growth the paper will treat in more detail the importance of stress and steps for the shape and lateral distributions of epitaxial crystals using several examples - (Co/W(100), Si(100): B, Au/W(110), Au/Mo(110), Cu/Mo(110), Co/W(110)) which have been studied with LEEM and/or spin-polarized LEEM (SPLEEM).

1. Introduction

Epitaxial nanostructures, in particular those which exhibit self-organization, are gaining increasing importance. Their formation is determined in part by kinetics, in part by energetics. At low temperatures kinetics, such as surface diffusion and attachment rates are dominating which is amply demonstrated by numerous STM studies and computer simulations of surface diffusion-limited aggregation or by STM studies of the low temperature growth of Si on Si(100). The resulting crystal sizes and shapes are usually beyond the reach of LEEM whose practical resolution is presently about 10nm. LEEM is, however, well suited for studies at higher temperatures at which kinetic effects decrease in importance and film growth is increasingly determined by energetics. This growth range is the subject of this paper in which it is assumed that nucleation and growth are not limited by diffusion or attachment problems. The emphasis will rather be on the influence of stress and steps. Beforehand a cautioning remark is appropriate: even if there are no surface diffusion limitations, surface diffusion can have a strong influence on the crystal shape. This is illustrated by the growth of "ashtray" crystals, observed recently in the system Pb/Si(100) [1] but seen already earlier in other systems [2, 3]. The explanation of this phenomenon is quite simple: the edge of the growing crystal receives a much larger supply of atoms from the two-dimensional Pb gas phase on the top of the probably mixed [4] PbSi adsorption layer than the center of the crystal does from the MBE source. The steps on the side faces of the crystal trap the arriving atoms so effectively that only a small fraction can contribute to the growth of the central part. This phenomenon has been known in the solution and electrolytic growth of 3d crystals for some time [5, 6] and should also occur frequently in epitaxy as long as the diffusion supply regions of neighboring crystals are large enough and do not overlap.

2. The Stressed Individual Crystal

A misfitting epitaxial crystal strained to fit a rigid substrate is an unstable configuration. The resulting stresses lead to strains both in the crystal and in the substrate. The associated strain energy [7] has to be taken into account in the minimization of the total energy of the crystal. This can be done by identifying the strain energy with the energy of the interface between crystal and substrate which depends then on its size and shape [8]. Although the minimization cannot be performed explicitly because of its mathematical complexity, the (110) oriented LiF crystals with large length to width ratios on NaCl(100) surfaces which were observed in one of the first electron microscopic studies of epitaxy [9] were explained in terms of this generalization of the Wulff construction. In the meantime the understanding of the influence of stress on the crystal shape has deepened considerably. For example, Tersoff et al.. [10] have given an elegant explanation for the large length to width aspect ratios of up to more than 50:1 of Ag crystals an Si(100) surfaces which have no interface anisotropy. Recently we have observed another striking case with extreme aspects ratio: Co on W(100), initially with RHEED [11] which subsequently was confirmed with LEEM [12] (Fig. 1). RHEED showed that the crystals grew in (11$\bar{2}$0)-oriented ribbons which were thin and high enough to produce excellent transmission

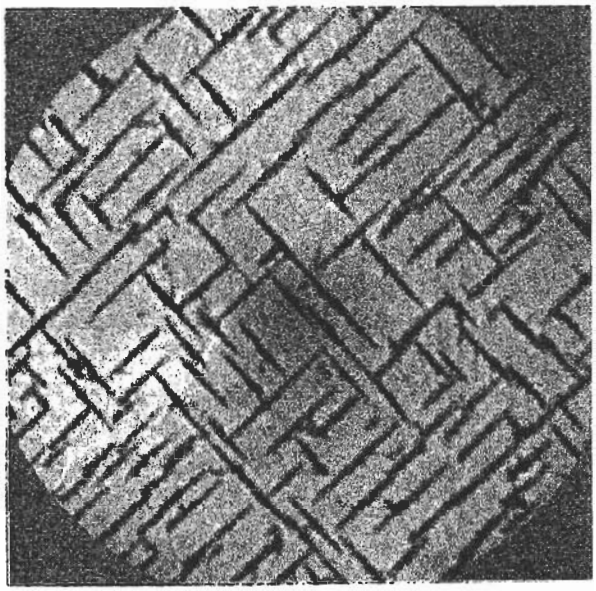

Fig. 1 LEEM image of Co ribbon crystals on W(110). Electron energy 8.3eV. Field of view 9μm [12].

patterns. In the LEEM images they appear as thin dark lines with two equivalent orientations, Co[0001] ‖ W[011] and [01$\bar{1}$]. The thickness of the ribbons in the RHEED transmission direction in which the misfit is large (Co[0001], 7.8%) is very small, so that these crystals escape detection by laterally averaging normal incidence surface analysis methods. The large aspect ratio is attributed to the small misfit (2.4%) in the direction along the ribbons (Co [1$\bar{1}$00]). These examples suggest that many such isolated "quantum wires" can be grown by selecting film-substrate combinations with the appropriate interfacial stress. In all cases the crystals were far enough apart so that their strain fields in the substrate did not overlap. The question what happens if this is no longer the case will be addressed next.

3. Crystal Distributions in Overlapping Strain Fields: The Striped Phase

The answer to this question was given in principle already 15 years ago by Marchenko [13] but did not achieve general attention until Alerhand's et al. [14] prediction of a striped phase for the equilibrium configuration of an ideal Si(100) surface. Their conclusion was that a single domain (2×l) or (1×2) surface is unstable to the formation of elastic-stress domains consisting of (2×l) and (1×2) stripes with alternating tensile and compressive stress normal to the stripes. This striped phase was, however, never observed on normal Si(100) surfaces. Only recent LEEM and STM studies of highly B-doped crystals[15] revealed the probable reason for this apparent failure of the theory: the stress anisotropy was apparently too low. Due to the fact that the Si-B bond length is shorter than the Si-Si bond length, B incorporated properly in the surface can increase this anisotropy considerably.

By controlling the B concentration in the surface via temperature-dependent B segregation the stripe periodicity could be varied over a wide range until its disappearance at high temperatures at which the monolayer islands assume the almond-shape observed in

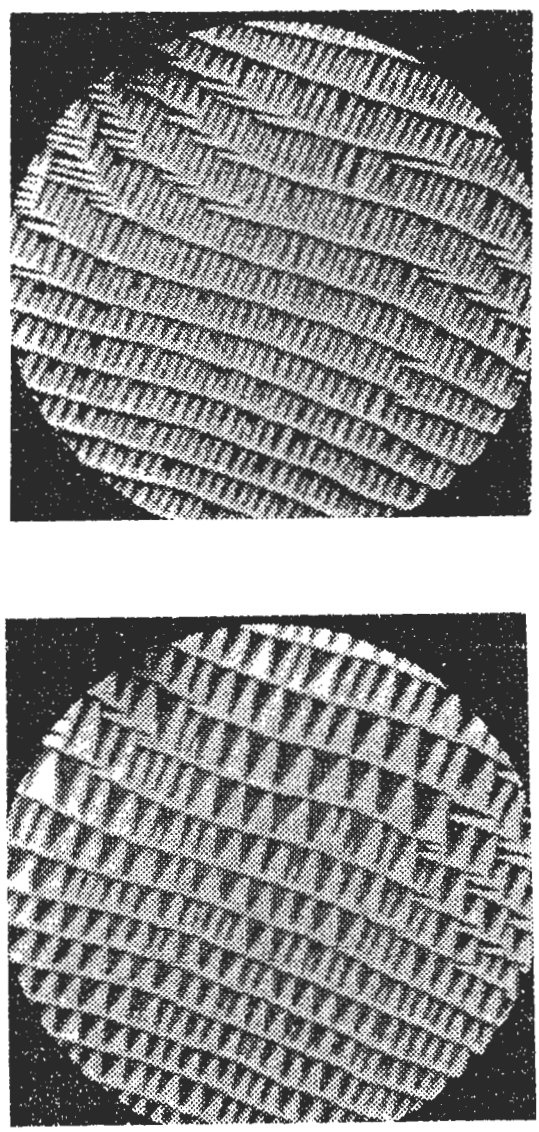

Fig. 2 LEEM images of the striped phase (a) and of the triangular-tiled structure (b) on B-doped Si(100). Electron energy 4.3eV. Field of view 7μm diameter [15].

previous growth studies close to equilibrium[16]. If the terraces are too narrow for the almonds to form, then the striped phase transforms via a triangular-tiled structure into the rough-smooth type S_B - type S_A step sequence of a clean surface at high temperatures (Fig. 2). The minimum stripe periodicity obtainable upon cooling depends upon the B concentration; in ref. [15] periodicities as low as 10 nm have been observed by STM.

The counterpart to the Si(100):B surface is the submonolayer system Au/W(110). On the basis of LEED diffractometry studies[17] and earlier LEEM observations of the submonolayer system Au/Mo(110)[18] it was predicted [19] that this system should also form a striped phase, a prediction which was recently confirmed by LEEM [12]. Fig. 3 shows some images taken at several temperatures at a fixed Au coverage of about 0.4 monolayers (ML). Contrary to the Si(100):B surface in Fig. 2 the stripe periodicity *de*creases with increasing temperature. This can be understood as follows: in the Si(100):B system the surface stress alteration between the two phases ((2×1) and (1×2)) *in*creases with increasing B concentration, that is *de*creasing temperature, in the Au/W(110) system the surface stress alteration between the two phases (Au-covered and free W) increases with *in*creasing mismatch, that is increasing temperature due to the difference in lateral thermal expansion of film and substrate which is evident from LEED diffractometry. The reverse temperature sequence is also evident in the appearance of the almond-shaped islands (on wide terraces) and the triangular islands (on narrow terraces) at low instead of at high temperatures (compare Figs. 2 and 3). At low (0.2 ML) and high (0.85 ML) coverages striped phases are formed as well, without any indication of a "droplet" or "inverted droplet" phase which have theoretically been predicted for less than about 0.3 ML [20, 21] and more than about 0.7 ML [20], respectively. The straightness of the Au/W(110) stripes, even at the highest temperatures at which the stripe pattern still can be resolved by LEEM, however, confirms the theoretical prediction of its stability against sinuousoidal displacements [20].

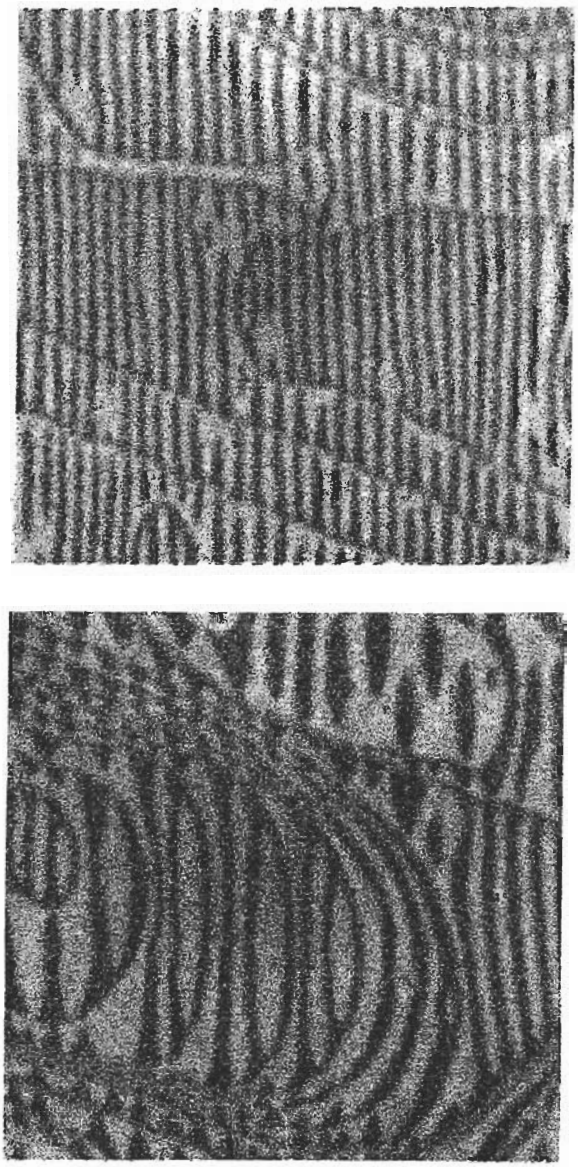

Fig. 3 LEEM images of the striped phase (a) of 0.4 ML Au on W(110) and its disappearance upon cooling due to the decreasing mismatch. Electron energy 7.2eV. Field of view 2×2μm² [12].

Although W and Mo differ very little in their lattice constants the striped phase of the submonolayer system Au/Mo(110) [18] is quite different: it appears in two domain orientations (∥ [1$\bar{1}$1], [1$\bar{1}\bar{1}$]) (Fig. 4) instead of only the one (∥ [001]) seen on W(110). Thus, small differences in the elastic properties of the substrate can cause significant changes in the domain pattern.

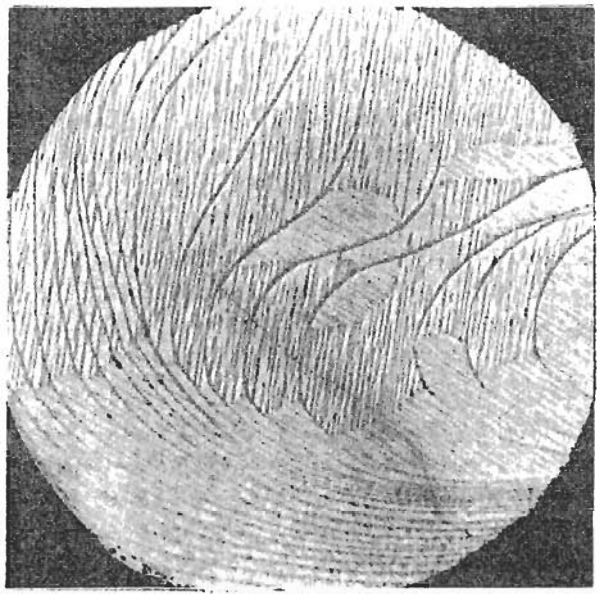

Fig. 4 LEEM image of the striped phase of submonolayer Au on Mo(110). Electron energy 14eV. Field of view 9μm diameter [18].

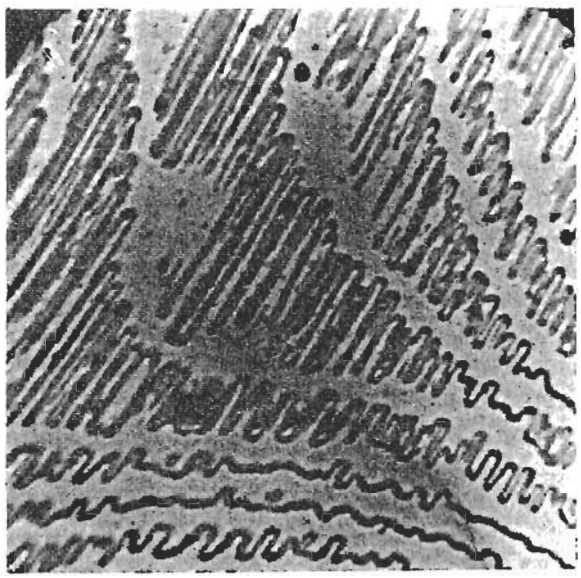

Fig. 5 LEEM image of the striped high temperature phase of 2 ML Cu on Mo(110). Electron energy 3eV. Field of view $4.3 \times 4.3 \mu m^2$ [22].

Striped phases occur not only in the submonolayer region. In the system Cu/Mo(110) which grows pseudomorphically up to 1 ML but subsequently forms a one-dimensionally misfitting double layer with reversible temperature-dependent structure, a striped phase forms at high temperature shortly before desorption of the second ML sets in. It is believed to involve also a restructuring of the substrate by breaking up the surface into stripes along the [001] direction (Fig. 5)[22]. These observations indicate that self-organization via substrate stress is not an exception but probably a rather common phenomenon which deserves a more thorough study than the mostly cursory work done up to now. Quantitative LEEM work under well-defined conditions should contribute significantly to the understanding of this interesting phenomenon useful for nanopatterning.

4. Substrate Steps in Heteroepitaxy

It is well established now that the first ML grows via step flow growth across each terrace, provided it is pseudomorphic, the temperature is high enough and the surface clean enough so that no 2d nucleation occurs. After one to several MLs the film usually acquires already a periodicity close to that of the bulk. The mismatch normal to the surface, that is the difference in the ML height between film and substrate, however, still can influence the film growth and properties. This will be illustrated by two examples. One is the terrace-limited layer-by-layer growth of Cu on Mo (110) [23]. Although the normal mismatch is only 6.6% it is an energetic penalty for a new nucleated ML on a given terrace to grow across a step onto a neighboring terrace. Steps seem to be no diffusion barriers under the growth conditions used. Therefore, the ML grows rapidly along the terrace, being fed by atoms from surrounding terraces on which no new ML is growing. If nucleation of new ML islands is statistical, a statistically rough surface consisting of atomically flat terraces of different height will form. If ML nucleation is preferred on a few terraces due to nucleation centers such as certain impurities very rough surfaces consisting of atomically smooth terraces with significant height differences may develop.

Fig. 6 LEEM (a) in-plane (b) and out-of-plane (c) magnetization SPLEEM images of 5 ML Co on W(110) Electron energy 3eV (a), 1.2eV (b). Field of view 6 μm diameter [12].

The second example [12] illustrates how a film property, its magnetic domain structure, may be influenced. Fig. 6a shows the topography of a 5 ML thick Co film on W(110). The three grey levels (bright, grey, dark) demarcate regions which are 3, 4 and 5 ML thick, respectively ("quantum size contrast"). The in-plane (Fig. 6b) and out-of-plane (Fig. 6c) magnetization SPLEEM images show no correlation of the domain walls with the Co ML steps but a clear correlation with the substrate steps which propagate through the Co layer. The normal mismatch between adjoining Co layers is 10%. This causes a high local strain and associated with it a local magnetic anisotropy which obviously encourages changes in the magnetization direction.

5. Conclusion

LEEM is an ideal tool for the study of isolated nanocrystals and of nanostructures with periodicities above about 20nm, in particular of their temperature dependence. Its monolayer depth resolution (step contrast) and thickness sensitivity (quantum size contrast) make LEEM/SPLEEM combined with LEED also uniquely useful for growth/structure/property correlations.

References

1. L. Li, C. Koziol, K. Wurm, Y. Hong, E. Bauer and I.S.T. Tsong, Phys. Rev. B 50 (1994) 10834.
2. S.Ino, private communication.
3. K. Yagi, private communication.
4. R.G. Zhao, J.F.Jia and W.S. Yang, Phys. Rev. B 48 (1993) 5333.
5. A.A. Chernov, Sov. Phys. Crystallography 8 (1963) 63.
6. Chr. N. Nanev, J. Cryst. Growth 140 (1994) 381.
7. J.H. van der Merwe, Proc. Phys. Soc. (London) A 63 (1950) 616.
8. E. Bauer, Z. Kristallogr. 110 (1958) 372.
9. E. Bauer, Z. Kristallogr. 110 (1958) 395.
10. J. Tersoff and R.M. Tromp, Phys. Rev. Lett. 70 (1993) 2782.
11. H. Wormeester, E. Hueger and E. Bauer, Phys. Rev. B, 54 (1996) 17108.
12. T. Duden, Ph.D. thesis, TU Clausthal 1996.
13. V.I. Marchenko, JETP Lett. 33 (1981) 381.
14. O.L. Alerhand, D. Vanderbilt, R.D. Maede and J.D. Joannopoulos, Phys. Rev. Lett. 61 (1988) 1972.

15. D.E. Jones, J.P. Pelz, Y. Hong, E. Bauer and I.S.T Tsong, Phys. Rev. Lett. 77 (1996) 330.
16. W. Swiech and E. Bauer, Surf. Sci. 255 (1991) 219.
17. N. Georgiev, Ph.D. thesis, TU Clausthal 1996.
18. M. Mundschau, E. Bauer, W. Telieps and W. Swiech, Surf. Sci. 213 (1989) 381.
19. E. Bauer, in Thin Films and Phase Transitions on Surfaces, ed. by M. Michailov and I. Gutzow, (Inst. Phys. Chem. Bulg. Acad. Sci., 1994), p. 47.
20. K.-O. Ng and D. Vanderbilt, Phys. Rev. B 52 (1995) 2177.
21. P. Zeppenfeld, M.A. Krzyzowski, Ch. Romainczyk, R. David, G. Comsa, H. Roeder, K. Bromann, H. Brune and K. Kern, Surf. Sci.
22. M. Mundschau, E. Bauer and W. Swiech, Catalysis Lett. I (1988) 405.
23. M. Mundschau, E. Bauer and W. Swiech, J. Appl. Phys. 65 (1989) 583.